

# Fast Star Pattern Recognition Using Spherical Triangles

Craig L. Cole\*

*Orbital Sciences Corporation, Dulles, VA 20166*

John L. Crassidis†

*University at Buffalo, State University of New York, Amherst, NY 14260-4400*

A current method by which star trackers identify stars is to match the angles between stars within its field of view to angles stored in a catalog. If an angle can be matched to one pair of stars, the attitude of the star tracker can be determined. However, the measurement of the angle will include error, and so the true angle can only be known to lie within a certain measured range. The result is, after comparing the measured angle to the catalog of angles, more than one pair of stars can be the correct solution. A method for narrowing down to one solution involves employing many angles within the field of view in a certain order, called “pivoting,” which can be time consuming and does not always yield a solution. The method presented here matches spherical triangles made from sets of three stars within the field of view to spherical triangles stored within a catalog. By using both the area and polar moment properties of the spherical triangle, the range of possible solutions is very quickly narrowed, fewer pivots to other spherical triangles are required, and the method is more likely to yield the correct solution than the angle method.

## I. INTRODUCTION

### A. STAR ID METHODS

A very important device on any spacecraft is the one which determines the spacecraft’s attitude. There are many different methods by which attitude can be determined, but one of the mostly widely used is the star tracker. Other methods for determining attitude exist, including sun sensors and magnetometers, but cannot report attitude with the precision a star tracker can. At best, a sun sensor-magnetometer system can only report attitude within 0.1 deg, while star trackers are capable of arc-second accuracy. Often, on high-budget missions, these other sensors will complement or back-up a star tracker. On missions with tight attitude knowledge requirements, the star tracker is often trusted to determine attitude completely on its own. Before an attitude can be determined, the stars within a tracker’s field of view (FOV) must be identified. If it can identify at least two stars, the attitude of the star tracker can be determined, which then can be transformed to the attitude of the spacecraft to which it is attached. The spacecraft can use this information to check its heading, make course changes or even recover from a “lost-in-space” condition.

The technology behind star trackers has changed much over the years. Evolving from gimballed to direct-head, the latest star trackers now use charge-coupled devices (CCD) for imaging, which offer high accuracy.<sup>1</sup> Still, they are not perfect devices since measurement errors will always exist. Even the small amount of error that exists in the image measurement of the stars within the star tracker’s FOV makes identifying the stars a very challenging problem. As a result, there are many different methods for identifying the stars within the FOV. One well known method involves measuring the angular separation between stars in the star tracker FOV, which attempts to match them to angles within a catalog of angles between stars.<sup>2</sup> This is called the “angle method” and has been the basis for many star recognition algorithms. It does not rely on other sensors for assistance, and can be used in a lost-in-space condition. Magnitude can also be used

---

\*ACS Engineer, Space Systems Group, Cole.Craig@orbital.com, Member AIAA.

†Associate Professor, Department of Mechanical & Aerospace Engineering, johnc@eng.buffalo.edu, Associate Fellow AIAA.

to help identify stars, but this is not simple when CCD's are used. For instance the CCD's sensitivity to different spectra of light must be understood and accounted for.<sup>3</sup> Other methods attempt to use "a priori" information to help the star tracker to determine the stars within its FOV.<sup>2,4-9</sup> Methods based on knowing the attitude of the spacecraft at an earlier point in time would not be suitable for lost-in-space conditions. Even neural networks are being tested for their potential to recognize stars within the star tracker's FOV.<sup>10</sup> It can be seen that the "perfect" star pattern recognition algorithm does not yet exist and the field is wide open for new methods.

The method presented here is called the "spherical triangle method." It uses spherical triangles from the stars in the FOV and compares them to a catalog of spherical triangles to find a match. It too has its roots in the angle method, which will be used as a basis for comparisons purposes to the spherical triangle method. To make the testing of both methods realistic, a "typical" star tracker has been chosen as a model. The Ball CT-601 star tracker has an  $8 \times 8$  degree FOV and can see down to magnitude 6.0 stars.<sup>4,11</sup> The testing model created here assumes an 8 degree circular FOV for simplicity, but the star pattern recognition algorithms tested can be applied to square fields of view.

## B. DESIGN THEORY

The importance of star trackers on spacecraft is difficult to overestimate. Errors in attitude knowledge can result in damage to or the complete loss of a spacecraft. An ideal star tracker would be able to report attitude instantly without chance of error in lost-in-space conditions and without aid from other sensors. In addition, it would require little in the way of computer resources such as storage and CPU speed. These are certainly conflicting constraints, and decisions have to be made when designing the star tracker as to what is most important.

For the methods presented here, rate of success and speed are given the highest priorities in the design of the algorithms. A star tracker's ability to report attitude quickly is desirable in situations where the spacecraft is tumbling; if the result lags too far behind the actual attitude of the spacecraft, the spacecraft may become very difficult to control. The idea behind the spherical triangle method is that by using more than one property to recognize a pattern of stars, it is more likely to reach the correct solution and do it using fewer stars. By comparison, the angle method can only use one property, the angle itself, for pattern matching and as a result will not approach a solution as quickly. Time measurements comparing both methods will be made to show this.

The penalty for success and speed is storage. It will be seen that the database used with the spherical triangle method is quite large when compared to that required for the angle method. It is only large by spacecraft standards, however; the database would easily fit onto a keychain-sized flash drive. The computer hardware used in spacecraft is designed to withstand the harsh environment of space, and as a result lag years behind the current state of the art in processor speed and storage. The technology continues to evolve, however, and tasks that are too demanding of spacecraft hardware today will likely be practical in the not too distant future.

## II. ANGLE METHOD

There are many methods by which a star tracker can determine what stars are within its FOV, many of which are proprietary. A well-known method involves matching the angle of separation between pairs of stars within the FOV to a catalog containing all of the angles between stars in the celestial sphere which can fit within the star tracker's FOV.<sup>2</sup> For instance, a circular 8 deg FOV star tracker would require a catalog of all the angles between stars in the celestial sphere 8 deg or less. If the measured angle can be matched to a single angle in the catalog, the stars that make up the angle would be known and so then would the attitude of the spacecraft.

To create the catalog of angles, a data structure called a spherical quad-tree is used.<sup>12</sup> A quad-tree structure is typically used to store objects located in 2-D space in such a way that objects can be found within a certain area without examining each and every object. The spherical quad-tree used here to catalog the angles enables cataloging angles in such a way that only each star's neighbors within a certain distance have to be examined to see if the angle between them is small enough to fit within the star tracker FOV. It greatly reduces the total number of pairs that needs to be examined and greatly reduces the time required to create the catalog. For the star tracker modeled here, the catalog created contains 106,308 angles and

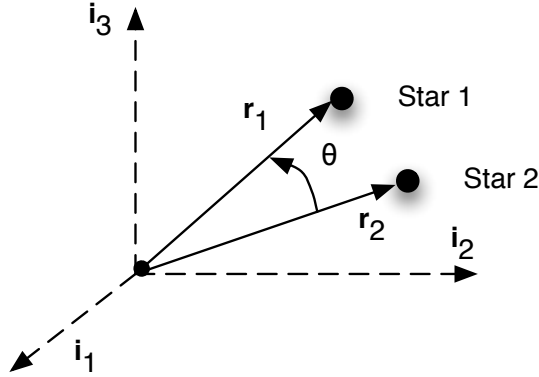


Figure 1. Angle Between Stars Used to Determine Attitude

occupies 12 MB of memory.

Once the angles are cataloged, they are sorted by angle. To make finding all the angles that lie within a given range fast, a technique called the “ $k$ -vector” approach is used.<sup>13</sup> If the angle of each pair of stars is plotted against its location in the catalog, a line can be drawn connecting the first and last pair of stars. The equation of this line can be used in association with the generated  $k$ -vector to locate where in the catalog a particular pair of stars with a given angle is located. This greatly reduces the computational burden since the star pattern search algorithm requires a search of the pairs of stars only within a measurement uncertainty region, not a search of the entire catalog.

### A. ANGLE BETWEEN TWO STARS

The angle between the vectors pointing to the stars is given by

$$\theta = \cos^{-1}(\mathbf{r}_1 \cdot \mathbf{r}_2) \quad (1)$$

where  $\mathbf{r}_1$  and  $\mathbf{r}_2$  are unit vectors pointing to each star, as shown in Figure 1. The vectors  $\mathbf{r}_1$  and  $\mathbf{r}_2$  are given in inertial space, however, only body measurements are known. Fortunately, the angle  $\theta$  is the same whether inertial vectors or body vectors are used. The problem is that the angle measured between the stars within the FOV of the star tracker will contain a certain amount of measurement error, which cannot be ignored. If the measurement follows a Gaussian distribution, its standard deviation can be determined and used to establish a range within which the true measurement is likely to lie. For instance, if the range is chosen to be the measurement angle  $\pm 3$  times the standard deviation of the measurement noise,  $3\sigma$ , then the true measurement is expected to be within this range 99.7% of the time.

### B. STANDARD DEVIATION OF ANGLE

The measurement error made by a typical modern-day star tracker follows a nearly zero-mean Gaussian white-noise process (for our simulations a standard deviation of 0.87 microradians of arc is used).<sup>14</sup> What will be needed for the angle method is the standard deviation of the angle between two stars when each star measurement possesses the error described. The standard deviation of the attitude-independent measurement, involving the dot product of two star vectors, can be used to provide a bound on the expected errors. We begin with the standard coordinate transformation equation:

$$\mathbf{b}_i = A\mathbf{r}_i \quad (2)$$

where  $\mathbf{r}_i$  is the direction of the star in Earth-Centered Inertial (ECI) coordinate system,  $A$  is the direction cosine matrix, which is orthogonal and proper, and  $\mathbf{b}_i$  is the direction of the star in the star tracker body coordinate system. When measurement errors exist, Shuster<sup>15</sup> has shown that nearly all of the probability

of the errors is concentrated on a very small area about the direction of  $A\mathbf{r}_i$ , so that the sphere containing that point can be approximated by a tangent plane, characterized by

$$\tilde{\mathbf{b}}_i = A\mathbf{r}_i + \mathbf{v}_i, \quad \mathbf{v}_i^T A\mathbf{r}_i = 0 \quad (3)$$

where  $\tilde{\mathbf{b}}_i$  denotes the  $i$ th measurement and the sensor error  $\mathbf{v}_i$  is approximately Gaussian, which satisfies

$$E(\mathbf{v}_i) = \mathbf{0} \quad (4a)$$

$$E(\mathbf{v}_i \mathbf{v}_i^T) = \sigma_i^2 [I - (A\mathbf{r}_i)(A\mathbf{r}_i)^T] \quad (4b)$$

where  $\sigma_i^2$  is the variance where  $E$  denotes expectation.

Taking the dot product of two body observations gives

$$\mathbf{b}_i^T \mathbf{b}_j = \mathbf{r}_i^T A^T A \mathbf{r}_j = \mathbf{r}_i^T \mathbf{r}_j \quad (5)$$

Equation (5) shows that the dot product is an attitude-invariant measurement. We now consider two body measurements with noise:

$$\tilde{\mathbf{b}}_i = A\mathbf{r}_i + \mathbf{v}_i \quad (6a)$$

$$\tilde{\mathbf{b}}_j = A\mathbf{r}_j + \mathbf{v}_j \quad (6b)$$

where  $\mathbf{v}_i$  and  $\mathbf{v}_j$  are assumed uncorrelated. Define the following effective measurement:

$$\begin{aligned} z &\equiv \tilde{\mathbf{b}}_i^T \tilde{\mathbf{b}}_j \\ &= \mathbf{r}_i^T \mathbf{r}_j + \mathbf{r}_i^T A^T \mathbf{v}_j + \mathbf{r}_j^T A^T \mathbf{v}_i + \mathbf{v}_i^T \mathbf{v}_j \end{aligned} \quad (7)$$

Since  $\mathbf{v}_i$  and  $\mathbf{v}_j$  are uncorrelated, then

$$E\{z\} = \mathbf{r}_i^T \mathbf{r}_j \quad (8)$$

Define the following variable:

$$\begin{aligned} p &\equiv z - E\{z\} \\ &= \mathbf{r}_i^T A^T \mathbf{v}_j + \mathbf{r}_j^T A^T \mathbf{v}_i + \mathbf{v}_i^T \mathbf{v}_j \end{aligned} \quad (9)$$

Then taking  $E\{p^2\}$  yields

$$\begin{aligned} \sigma_p^2 &\equiv E\{p^2\} \\ &= \mathbf{r}_i^T A^T R_j A \mathbf{r}_i + \mathbf{r}_j^T A^T R_i A \mathbf{r}_j + \text{Trace}(R_i R_j) \\ &= \text{Trace}(A\mathbf{r}_i \mathbf{r}_i^T A^T R_j) + \text{Trace}(A\mathbf{r}_j \mathbf{r}_j^T A^T R_i) + \text{Trace}(R_i R_j) \end{aligned} \quad (10)$$

where  $E\{\mathbf{v}_i \mathbf{v}_i^T\} \equiv R_i$  and  $E\{\mathbf{v}_j \mathbf{v}_j^T\} \equiv R_j$ . The last term is typically higher-order, which can be ignored. Also, if  $A\mathbf{r}_i$  and  $A\mathbf{r}_j$  are replaced by  $\tilde{\mathbf{b}}_i$  and  $\tilde{\mathbf{b}}_j$  respectively, then the variance is given by

$$\begin{aligned} \sigma_p^2 &\equiv E\{p^2\} \\ &= \tilde{\mathbf{b}}_i^T R_j \tilde{\mathbf{b}}_i + \tilde{\mathbf{b}}_j^T R_i \tilde{\mathbf{b}}_j + \text{Trace}(R_i R_j) \\ &= \text{Trace}(\tilde{\mathbf{b}}_i \tilde{\mathbf{b}}_i^T R_j) + \text{Trace}(\tilde{\mathbf{b}}_j \tilde{\mathbf{b}}_j^T R_i) + \text{Trace}(R_i R_j) \end{aligned} \quad (11)$$

Typically, errors introduced by this substitution are second-order in nature,<sup>15</sup> so the variance is completely independent of the attitude matrix  $A$ .

If  $R_i = \sigma_i^2 I$  and  $R_j = \sigma_j^2 I$ , which is valid for most star trackers, then

$$\sigma_p^2 = \sigma_i^2 + \sigma_j^2 + 3\sigma_i^2 \sigma_j^2 \quad (12)$$

Furthermore, if  $\sigma_i^2 = \sigma_j^2 \equiv \sigma^2$ , which is also valid for most star trackers, then  $\sigma_p^2 = 2\sigma^2 + 3\sigma^4$ . If  $\sigma$  is small, then the  $3\sigma^4$  term can be excluded. The variance of the angle between the stars is then

$$\sigma_p^2 = 2\sigma^2 \quad (13)$$

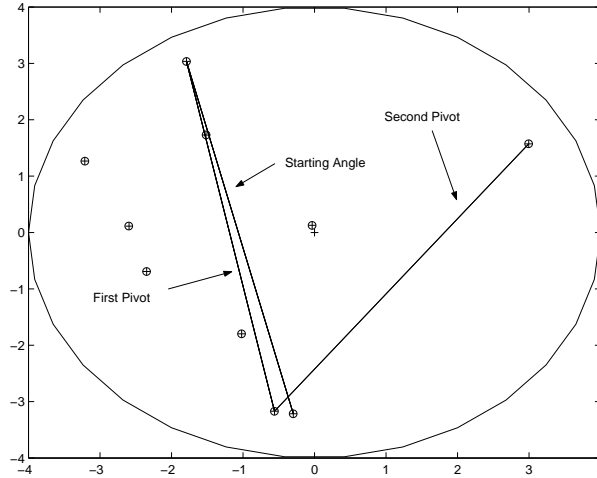


**Figure 2. Angle Method Pivoting Example**

The standard deviation of the angle measurement is then

$$\sigma_p = \sqrt{2}\sigma \quad (14)$$

Equation (14) is akin to the standard “root-two” increase in noise when adding two noisy signals, even though our case involves a dot product of two vectors.

The chosen  $\beta\sigma_p$  bound (for some scalar  $\beta$ ) has a large effect on the results of both the angle and spherical triangle methods. If the correct solution lies outside the bounds of the measurement error, neither method will find the solution, or worse arrive at an incorrect solution. If the  $\beta\sigma_p$  bound is set high, it is less likely an incorrect solution will be reached, since it is more likely the correct solution lies with the  $\beta\sigma$  bound. However, if the  $\beta\sigma_p$  bound is set too high, too many possible solutions will exist for each angle and spherical triangle in the FOV and a single solution may not be reached. Both methods are demonstrated using a  $3\sigma_p$  bound, meaning the probability that the correct angle will be within the range of the measured angle will be 99.7%.

### C. ANGLE PIVOT

If there exists more than one possible solution to a measured angle, one method by which the correct solution can be determined is based on “pivoting.” After all the possible solutions to the first angle are determined, a second angle within the FOV is selected such that it shares one star in common with the first angle. Once all the potential solutions to the second angle are found, the stars that make up both angles are examined. Since the solution to both angles must have a star in common, any angles on either list that do not have a star in common with at least one angle on the other list are rejected. If the number of possible solutions for each measured angle isn’t reduced to one after the elimination, another pivot is made; a third angle is chosen such that it has at least one star in common with the second angle, and the possible solutions for the second and third angles that do not share a common star are rejected.

The pivoting process continues until a single solution is reached or the star tracker runs out of angles to which it can pivot. If it runs out of angles before obtaining a single solution, then the result is inconclusive. An example of the pivoting process is shown in Figure 2. The large circle represents the star tracker’s FOV. The stars true locations are shown as small circles, while the measured positions are crosses. The two stars that offer the largest angle, which typically offer the fewest possible number of solutions, form the first angle examined. The two pivots that follow are indicated as well.

Ideally, the angles in the FOV should be ordered so that the angle with the fewest number of solutions is examined first. The second angle chosen should be the angle with the next-fewest number of combinations that shares one star in common with the first angle and so on. This method reduces the number of combinations that need to be examined and makes it more likely to reach a solution quickly. The effect of

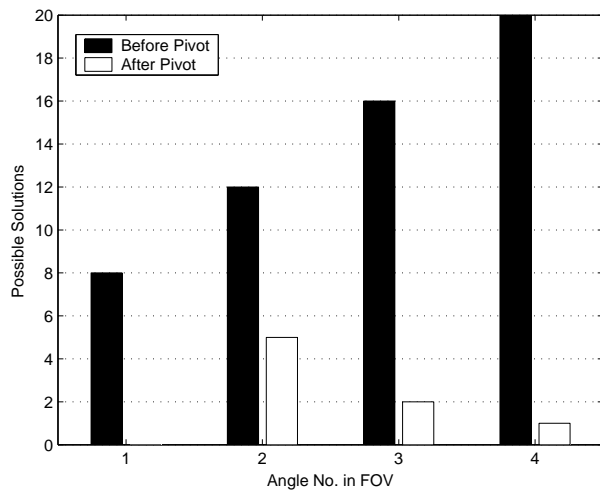


Figure 3. Effect of Pivoting on the Number of Solutions

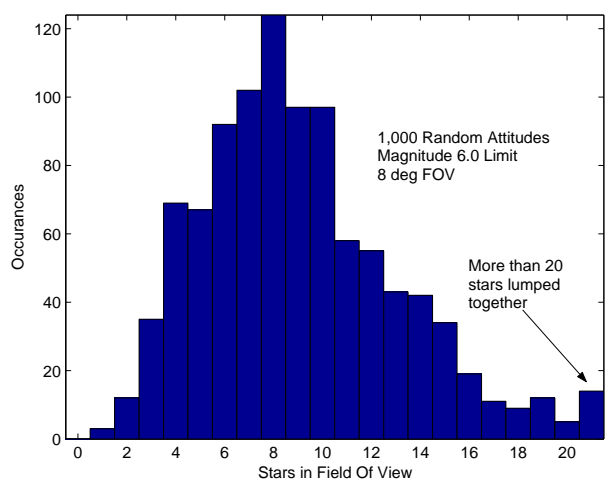


Figure 4. Distribution of the Number of Stars in the Field of View

pivoting in this manner is shown in Figure 3. Despite the number of solutions per angle increasing, typically, the number of solutions after comparing stars between each will drop eventually to one. In the figure, it shows that 3 pivots are required to reach a single solution. How many pivots can be made is a function of the number of stars within the FOV of the star tracker and the magnitude of stars to which it is sensitive. For a star tracker with an 8 deg FOV, sensitive down to magnitude 6.0 stars, a distribution of the number of stars that it will see for a large number of random attitudes can be plotted, which is shown in Figure 4. The largest number of occurrences involves 6 to 10 stars.

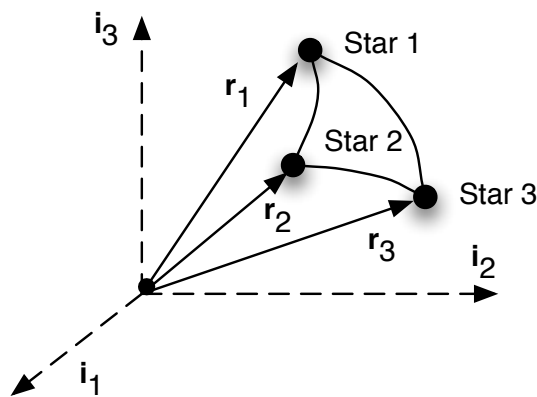


Figure 5. Spherical Triangles Used to Determine Attitude

### III. SPHERICAL TRIANGLE METHOD

Instead of measuring the angle between pairs of stars, the spherical triangle method creates spherical triangles of combinations of three stars, as shown in Figure 5. The idea is that more information can be obtained from a spherical triangle than an angle, which will enable a star tracker to determine the identity of stars more quickly and use fewer stars overall than the angle method. In the algorithm presented here, the area and polar moment of spherical triangles are used to determine what spherical triangle is being examined by the star tracker. One drawback of the spherical triangle method is that it will be impossible to identify stars with less than three stars in the FOV, while the angle method needs only two stars. However, after

including the measurement error present in the star tracker, under typical conditions with pivoting, more than two stars are required to arrive at a solution using the angle method. What will be shown is that the spherical triangle method will require fewer pivots than the angle method and will more likely yield a single solution using fewer stars overall.

While the angle catalog can be created using more straightforward methods than the spherical quad-tree, to create the spherical triangle catalog without it would have been difficult. Having to examine stars in combinations of three instead of two greatly increases the total number of tests to execute. The catalog suiting the star tracker modeled here contains 662,779 spherical triangles. For each of these triangles, the area and polar moment must be calculated making the catalog 167 MB in size, more than ten times larger than the equivalent angle catalog.

Like the angle method, the spherical triangles must be sorted by area and polar moment so that the  $k$ -vector approach can be used to locate spherical triangles quickly by their area or polar moment. So that two separate catalogs aren't necessary, two linked-list data structures are sorted instead of the spherical triangles themselves. In addition, plotting each spherical triangle's area against its position in the sorted list is not linear. To make the  $k$ -vector approach as fast as possible, a parabola is fit between the first and last points (more details can be found in Ref. 12).

## A. SPHERICAL TRIANGLE AREA

Given three unit vectors pointing toward three stars, the area of a spherical triangle can be found using the following equation:<sup>16</sup>

$$\mathcal{A} = 4 \tan^{-1} \sqrt{\tan \frac{s}{2} \tan \frac{s-a}{2} \tan \frac{s-b}{2} \tan \frac{s-c}{2}} \quad (15)$$

where

$$s = \frac{1}{2}(a + b + c) \quad (16a)$$

$$a = \cos^{-1} \left( \frac{\mathbf{b}_1 \cdot \mathbf{b}_2}{|\mathbf{b}_1| |\mathbf{b}_2|} \right) \quad (16b)$$

$$b = \cos^{-1} \left( \frac{\mathbf{b}_2 \cdot \mathbf{b}_3}{|\mathbf{b}_2| |\mathbf{b}_3|} \right) \quad (16c)$$

$$c = \cos^{-1} \left( \frac{\mathbf{b}_3 \cdot \mathbf{b}_1}{|\mathbf{b}_3| |\mathbf{b}_1|} \right) \quad (16d)$$

The equation is given for the star tracker frame, but can also be used in the ECI frame. To obtain a bound for the measurement error (replacing  $\mathbf{b}_1$ ,  $\mathbf{b}_2$  and  $\mathbf{b}_3$  with measured quantities), the standard deviation of the calculated area must be calculated.

## B. STANDARD DEVIATION OF AREA

The determination of the standard deviation of the area error for a spherical triangle made up of vectors containing measured quantities can be done using a linearization approach.<sup>17</sup> We start with a basic measurement equation:

$$\tilde{\mathbf{y}} = \mathbf{f}(\mathbf{v}) \quad (17)$$

where  $\tilde{\mathbf{y}}$  is the measurement and  $\mathbf{v}$  is a zero-mean noise process with covariance  $R$ . Expanding Eq. (17) using a first-order Taylor Series about the mean of  $\mathbf{v}$ , which is zero, gives

$$\tilde{\mathbf{y}} = \mathbf{y} + \left. \frac{\partial \mathbf{f}}{\partial \mathbf{v}} \right|_{\mathbf{v}=\mathbf{0}} \mathbf{v} \quad (18)$$

where  $\mathbf{y}$  is the truth. Defining  $\left. \frac{\partial \mathbf{f}}{\partial \mathbf{v}} \right|_{\mathbf{v}=\mathbf{0}} \equiv H$ , then the covariance of  $\tilde{\mathbf{y}}$  is given by

$$\begin{aligned} E\{(\tilde{\mathbf{y}} - \mathbf{y})(\tilde{\mathbf{y}} - \mathbf{y})^T\} &= H E\{\mathbf{v}\mathbf{v}^T\} H^T \\ &= H R H^T \end{aligned} \quad (19)$$

This approach is valid if the first-order Taylor series shown in Eq. (18) adequately models the process, which is valid for the star tracker measurement process since the signal-to-noise ratio is large.

Applying this approach to the spherical triangle area equation, which is a function of  $a$ ,  $b$  and  $c$  (the angles between the vectors toward the stars), is fairly complicated. However, a simple and mathematically equivalent approach can be used by noting that since the Taylor series expansion is about  $\mathbf{v} = \mathbf{0}$ , then the matrix  $H$  can be formed by taking partials with respect to  $a$ ,  $b$  and  $c$  directly. Hence,  $H$  is given by

$$H = \frac{4}{1+z^2} \begin{bmatrix} \frac{dz}{da} & \frac{dz}{db} & \frac{dz}{dc} \end{bmatrix} \quad (20)$$

where

$$z = \sqrt{\tan\left(\frac{s}{2}\right) \tan\left(\frac{s-a}{2}\right) \tan\left(\frac{s-b}{2}\right) \tan\left(\frac{s-c}{2}\right)} \quad (21)$$

and

$$\frac{\partial z}{\partial a} = -\frac{u_1 - u_2 + u_3 + u_4}{8z} \quad (22a)$$

$$\frac{\partial z}{\partial b} = -\frac{u_1 + u_2 - u_3 + u_4}{8z} \quad (22b)$$

$$\frac{\partial z}{\partial c} = -\frac{u_1 + u_2 + u_3 - u_4}{8z} \quad (22c)$$

where

$$u_1 = \left[ \cos^2\left(\frac{a+b+c}{4}\right) \right]^{-1} \tan\left(\frac{b+c-a}{4}\right) \tan\left(\frac{a+c-b}{4}\right) \tan\left(\frac{a+b-c}{4}\right) \quad (23a)$$

$$u_2 = \tan\left(\frac{a+b+c}{4}\right) \left[ \cos^2\left(\frac{b+c-a}{4}\right) \right]^{-1} \tan\left(\frac{a+c-b}{4}\right) \tan\left(\frac{a+b-c}{4}\right) \quad (23b)$$

$$u_3 = \tan\left(\frac{a+b+c}{4}\right) \tan\left(\frac{b+c-a}{4}\right) \left[ \cos^2\left(\frac{a+c-b}{4}\right) \right]^{-1} \tan\left(\frac{a+b-c}{4}\right) \quad (23c)$$

$$u_4 = \tan\left(\frac{a+b+c}{4}\right) \tan\left(\frac{b+c-a}{4}\right) \tan\left(\frac{a+c-b}{4}\right) \left[ \cos^2\left(\frac{a+b-c}{4}\right) \right]^{-1} \quad (23d)$$

Solving for the variance of the area (denoted by  $\sigma_{\mathcal{A}}^2$ ) gives

$$\sigma_{\mathcal{A}}^2 = \sigma^2 H H^T \quad (24)$$

Note that the matrix  $H$  is evaluated at the respective true values; however, replacing the true values with the measured ones leads to second-order errors that are negligible. Since the standard deviation,  $\sigma_{\mathcal{A}}$ , is derived analytically, the bounds over which the true area is likely to exist can be determined precisely, no matter the shape or size of the spherical triangle.

### C. SPHERICAL TRIANGLE POLAR MOMENT

The polar moment makes a good counterpart to area, since it is possible for two spherical triangles that have the same area to have very different second moments. In addition, two spherical triangles that have the same polar moments may have very different areas. When it comes time to match spherical triangles seen within the FOV of the star tracker to spherical triangles in the catalog, use of these two approaches will rapidly reduce the number of possible solutions.

The polar moment of the triangle about its centroid is calculated by breaking the triangle into smaller triangles. The area of each of the smaller triangles,  $d\mathcal{A}$ , is multiplied by the square of the arc distance from the centroid of each smaller triangle to the centroid of the overall triangle. The result of each smaller triangle is then summed:

$$I_p = \sum \theta^2 d\mathcal{A} \quad (25)$$

Note that the polar moment can also be calculated using attitude independent measurements. A recursive algorithm is used to determine the area, breaking each spherical triangle into four smaller triangles until a

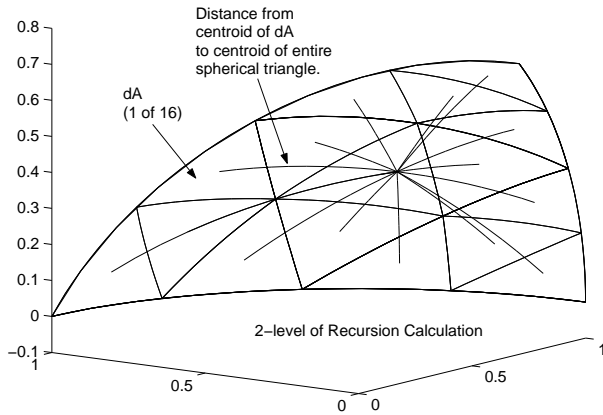


**Figure 6. Method for Calculating the Polar Moment of a Spherical Triangle**

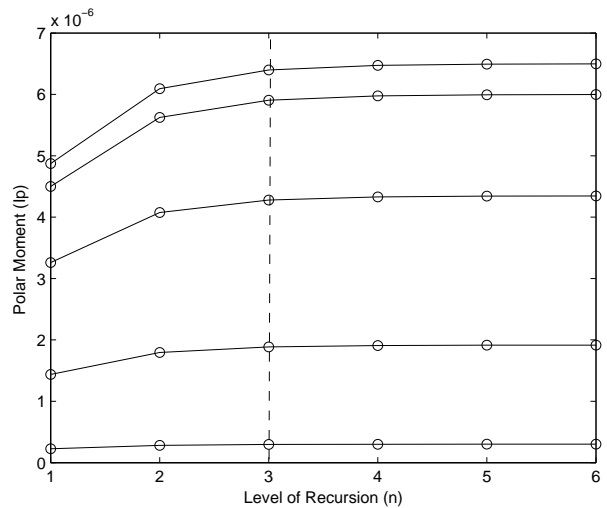


**Figure 7. Convergence of Polar Moment Recursive Algorithm**

target depth of recursion is met, which is shown using a sample spherical triangle in Figure 6. Since the accuracy of the method depends on how many triangles the original triangle is broken into, it is important to determine how many levels of recursion are required to achieve a good approximation of the actual solution. An algorithm has been written to randomly select spherical triangles from the catalog and determine the polar moment using different levels of recursion. The results are shown in Figure 7. It can be seen that three levels of recursion, where each triangle is broken into  $4^3$  or 64 pieces, are relatively close to the values at which each converged. Therefore, only three levels of recursion are used throughout the routines.

#### D. POLAR MOMENT STANDARD DEVIATION

Unlike the area case, the standard deviation of the second moment calculation is difficult to compute analytically. We choose to find a bound through simulation. A thousand random triangles from the catalog are chosen and one hundred measurements of the second moment for each triangle are made, including random measurement error. Figure 8 shows how the standard deviation of the measurements varies as a function of the polar moment of the triangle. What can be seen is triangles with similar polar moments may have a different standard deviation when the same amount of random error is included in the measurements. To put a bound on the measurement error, a line is drawn slightly above the maximum standard deviations on the chart. Clearly, this is a very conservative approach. Hence, it is safe to say that the standard deviation of any second moment measurement will lie under this line, and will ensure, for instance a  $3\sigma$  bound, the probability that the true measurement will be within the bounds at least 99.7% of the time.

#### E. SPHERICAL TRIANGLE PIVOT

The method for matching spherical triangles is similar to the method for matching angles. A spherical triangle is made from three stars in the FOV and its area and polar moment are calculated. A range over which the true area and polar moment exist are calculated using the standard deviations for each. Going through the catalog, triangles that have an area and polar moment that fit within the bounds calculated for the triangle in the FOV are tabulated. Ideally, only one possible solution remains, but this typically does not happen. When more than one solution exists, a pivot similar to the angle method is made. Another spherical triangle is made from the stars in the FOV such that there are two stars in common with the first triangle, as shown in Figure 9. A list of possible solutions is made and then the solutions between the first spherical triangle and second spherical triangle are compared. Any solution in each list that does not have two stars in common with at least one solution in the other lists is discarded. After the comparison is made, if more than one solution exists, another pivot is made. Pivoting continues until either a single solution is found or there are no more spherical triangles with which to pivot. Pivoting such that only one star is

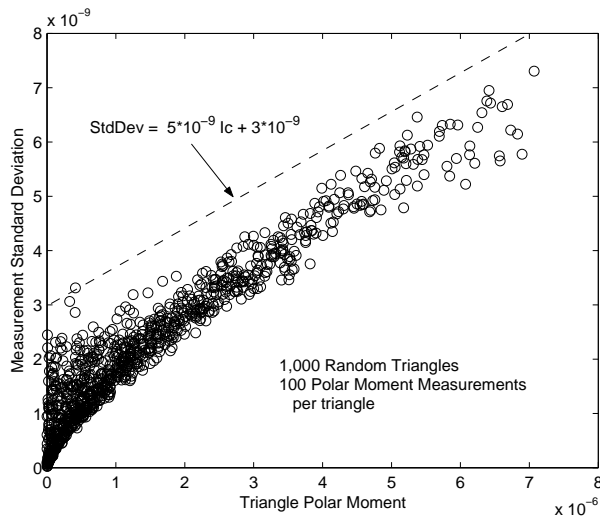


**Figure 8. Standard Deviation as a Function of Spherical Triangle Polar Moment**

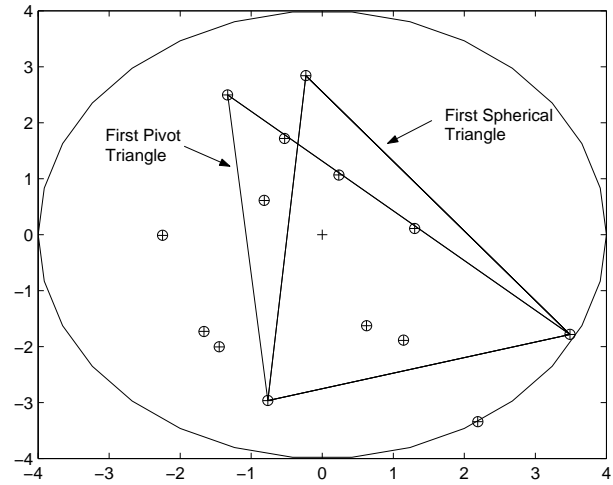


**Figure 9. Stars Within Star Tracker's Field of View**

shared between the first and second spherical triangles can be done, but would be less effective. The number of spherical triangles that are likely to share one star is greater than two, so the solution would require a greater number of pivots.

Testing each possible solution to the first spherical triangle against each possible solution in the pivot triangle can be time consuming, since there can be hundreds of solutions per triangle in the FOV. To reduce the number of combinations to test, three binary search trees are created.<sup>12</sup> The first tree contains star number 1 of each of the first triangle's possible solutions. The second tree contains star number 2, and tree number three contains star number 3. One of the pivot triangle's stars are checked to see if it exists in any of the three binary trees, and if it does, it tests the other two stars to see if it matches any of the stars of the triangle it matched in the binary tree. If not, a second star is tested against the binary trees, similar to the first. If still nothing matches, that triangle can be excluded as a solution. This approach greatly reduces the number of overall combinations that need to be tested, which greatly improves the speed of the algorithm.

## IV. COMPARISON OF METHODS

To test the angle and spherical triangle methods, a random star tracker attitude is generated 1,000 times. Each method is tested to see if it can positively identify at least one angle or spherical triangle in the FOV. The star pattern recognition algorithm does not attempt to determine final attitude; it only identifies the stars that make up the angles or triangles. If all of the stars determined in the star tracker's FOV by the star pattern recognition algorithm actually are in the FOV, it is considered a correct result. If any of the stars outputted by the algorithm are not in the FOV, the result is considered a failure. If the algorithm cannot positively identify any of the stars in the FOV, it is recorded as an inconclusive result. Under ideal conditions, a star tracker will only see stars within its boresight. However, it is entirely possible a piece of space debris enters a tracker's FOV, which may be misinterpreted as a star. Both the angle method and the spherical triangle method will be tested to see how such a "false" star affects the ability of each algorithm to reach a solution.

### A. STAR TRACKER RANDOM ATTITUDE

Each time the star pattern recognition algorithm is tested, the simulated star tracker must be set in a random attitude and the stars within the FOV determined. The locations of the stars then have to be mapped to the star tracker body frame to demonstrate that the properties of the triangles cataloged are not dependent on the attitude in which the triangles properties have been calculated. Given the body axis in terms of the tracker coordinate frame, the location of the stars in the ECI coordinate frame can be converted to the

frame of the star tracker using Eq. (2) with a random attitude.<sup>18</sup> The coordinates of the stars are so far still true, which would not be reported by a real star tracker. A measurement error with a standard deviation of 87 microradians is added to the true body vectors. This is done by adding a Gaussian random vector to the true vector, then making the resultant a unit vector. This results in a distribution that is not perfectly Gaussian, however, this approach is valid to within first-order and can be used for simulation purposes. If a false star is added to the FOV, then another random frame is created such that the 1-axis is collinear with the boresight of the tracker. Either of the two remaining axes is perpendicular to the boresight, and so a vector is created along one of the axes with a random length up to half the FOV of the tracker. The false stars' direction in ECI coordinates is then the boresight vector plus the random vector unitized. The vector is then converted to the frame of the star tracker and noise added as if it were another star. This false star is then added to the list of stars seen in the FOV of the star tracker and used in either the angle or spherical triangle method for solution.

## V. TESTING CONDITIONS

The CPU times stated are based on the hardware and software used, shown in Table 1. All graphics output from the routines are turned off and care is taken to ensure there are no other significant processes running in the background during testing. Each method is reduced to a single subroutine called from the random attitude testing routine. The time is measured from the line of code directly before calling the routine to the time it returns from it. The MATLAB<sup>®</sup> variable “CPU TIME” is used. Both the angle and spherical triangle method star pattern recognition algorithms are run with only one limit: if the number of possible solutions to any particular angle or triangle exceeds 10,000, then the angle or triangle is rejected. Despite the effort to make the code as fast as possible, the time required for this solution far exceeds most other solutions and does not significantly contribute to successful results.

**Table 1. Hardware and Software Used for CPU Time Measurements**

Item
Apple Powerbook G4, 500 MHz, 512 MB RAM
Apple OS X, Version 10.3.2
Apple X11, Version 1.0
Matlab Version 6.5.0.1951, Release 13

## VI. ANGLE METHOD RESULTS

### A. OVERALL SUCCESS RATE

Referring to Figure 10 it can be seen that the angle method is successful in identifying at least one angle in the FOV only 57% of the time and cannot positively identify any of the angles 42% of the time, even when allowed virtually unlimited pivots. Less than one percent of the attitudes tested contained less than two stars within the FOV, for which the angle method could not be tested and less than one percent of the attitudes give incorrectly identified results. Since every possible triangle has been cataloged, the only way an incorrect result can occur is if the correct solution lies outside the  $3\sigma$  bound placed on the angle recognition algorithm. Since the probability of the angle being within a  $3\sigma$  bound is 99.7%, the errors encountered are not unexpected.

Referring to Figure 11, it can be seen that the angle method does not work if there are less than 3 stars in the FOV. This implies that at least one pivot is required before any stars can be identified. Even with three stars in the FOV, the angle method yields a solution only a small fraction of the time. Once four stars are present in the FOV, the angle method begins to show significantly more success. If four stars are present, the angle method is successful 75% of the time and becomes more successful as more stars enter the FOV. But the rate of success drops again after 7 stars. Graphs summarizing the results are shown in Appendix A.

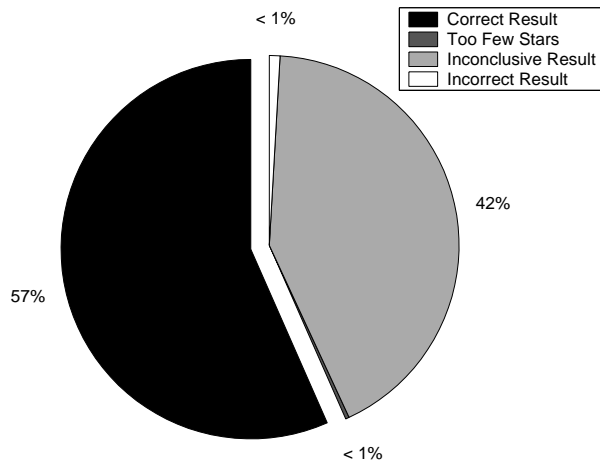


Figure 10. Overall Results for Angle Method without Pivot Limit

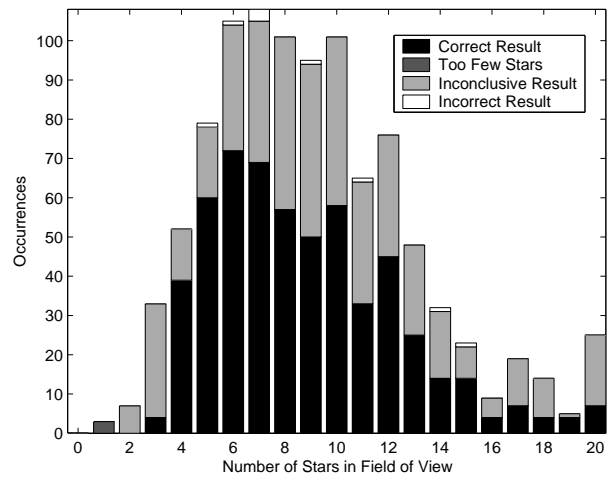


Figure 11. Distribution of Results for Angle Method without Pivot Limit

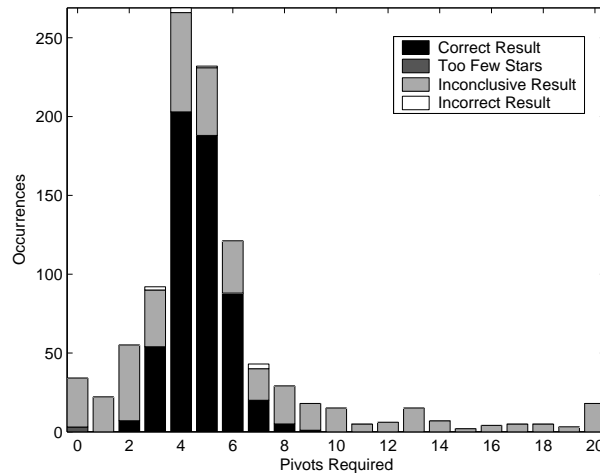


Figure 12. Pivots Required for Angle Method without Pivot Limit

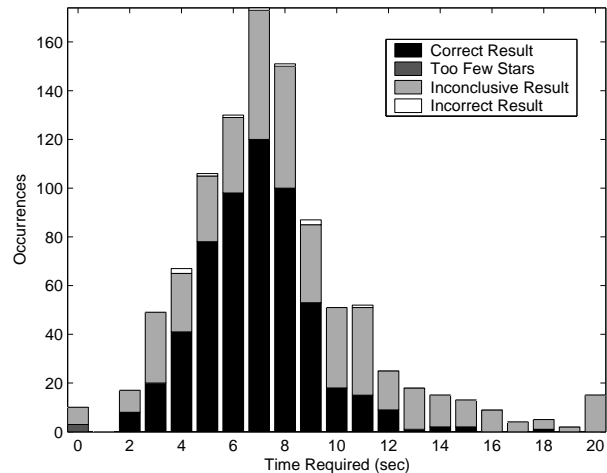


Figure 13. CPU Time Required for Angle Method without Pivot Limit

## B. PIVOTS REQUIRED

The number of pivots required by the angle method is shown in Figure 12. The average number of pivots is 5.48, with a standard deviation of 4.41, including the short spike at the left side of the chart. This spike is produced since no pivoting occurs if there are less than 3 stars in the FOV. Because the angle method requires two stars before pivoting, the average number of stars required is 7.48.

It is important to note that any attitude that requires nine or more pivots would ultimately not be solved. The angle method attempts pivots from largest angle to smallest angle, since the largest angles tend to have the smallest number of possible solutions. After a certain number of pivots, the number of possible solutions for an angle becomes so great that pivoting no longer reduces the possible number of solutions. In some cases, the number of solutions can begin to rise. In addition, the angle method will not yield a correct result if it has not achieved a correct result within nine pivots. Thus, the time efficiency of the method may be improved by limiting the maximum number of pivots to nine.

## C. CPU TIME REQUIRED

The CPU time required to execute the angle method is shown in Figure 13. The average time required is 7.67 seconds, with a standard deviation of 3.60 seconds. As with the pivot chart, this chart shows a short

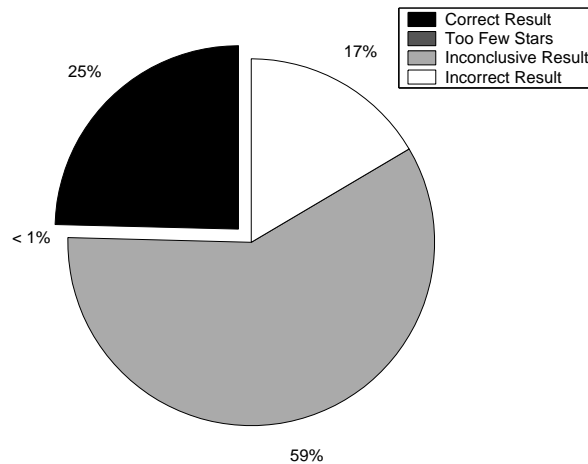


Figure 14. Angle Method Results With a False Star in the FOV

spike at the left side, resulting from requiring at least 3 stars in the FOV before a pivot can be made. Since no pivots can be made in those situations, little CPU time is required. Another spike exists at the right side of the chart. All the attitudes requiring more than 20 seconds are grouped together to make the chart more compact.

Since a significant amount of time is spent by the angle recognition algorithm determining the order for pivoting, the time results can be improved by limiting the number of pivots which the algorithm can take. It has been shown in the last section that if an attitude requires more than nine pivots, then a solution cannot be found, so the algorithm has been tested limiting the number of pivots to nine. Graphs summarizing the results are shown in Appendix B. The overall success rate remains 55%, but the average time required per attitude dropped to 6.89 seconds, a 10% improvement. The standard deviation also drops to 2.37 seconds. Since the number of pivots is limited, the average number of pivots required drops to 4.86, and therefore the number of average number of stars required drops to 6.86.

#### D. FALSE STAR INCLUSION

If a false star is added to the FOV, the angle method has a much more difficult time reaching a solution, as shown in Figure 14. The overall success rate drops to 25% and 17% of the results are incorrect. If the pivot order happens to include the false star, the angle method cannot reach the correct result and will either approach the wrong solution or no solution at all. Graphs summarizing the results are shown in Appendix C.

## VII. SPHERICAL TRIANGLE METHOD RESULTS

### A. OVERALL SUCCESS RATE

The overall results for the spherical triangle method are shown in Figure 15. This method is able to obtain a successful result 92% of the time, but is not able to positively identify any spherical triangles 7% of the time. Less than one percent of the attitudes contained less than 3 stars in the FOV and had little impact overall. In addition, less than one percent of the attitudes are incorrectly identified, which is to be expected due to the  $3\sigma$  bound placed on the spherical triangle search.

The overall result as a function of the number of stars present in the FOV is shown in Figure 16. This method cannot be used when there are less than three stars in the FOV and is never able to determine any of the triangles in the FOV with less than four stars, meaning that at least one pivot is always required. Once there are four stars in the FOV, the spherical triangle method is capable of recognizing at least one of the triangles 73% of the time. If there are at least four stars in the FOV, the spherical triangle method will arrive at the correct solution 92% of the time; if there are five or more stars in the FOV, the correct solution

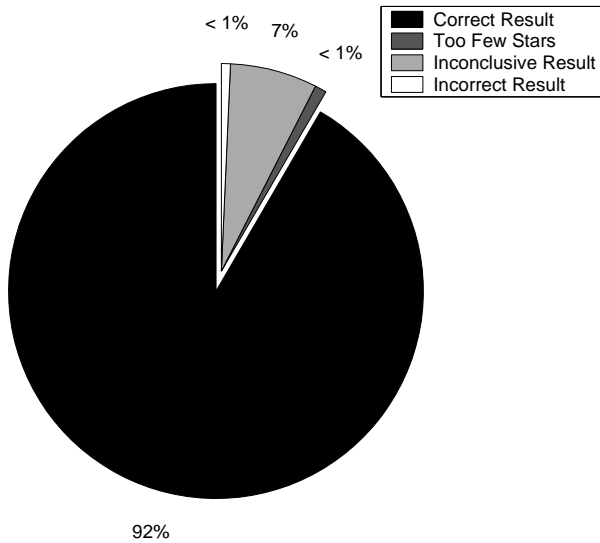


Figure 15. Overall Results for Spherical Triangle Method without Pivot Limit

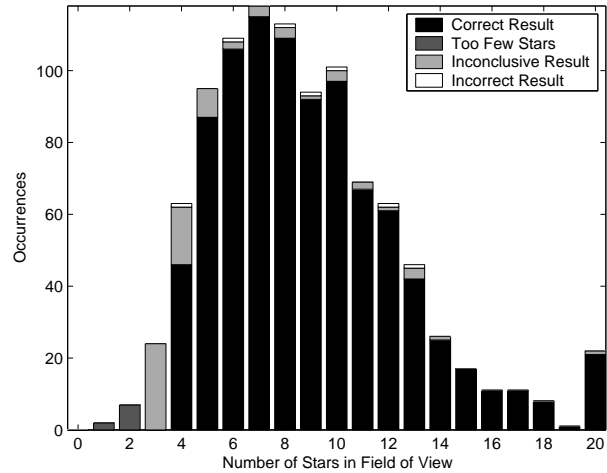


Figure 16. Distribution of Results for Spherical Triangle Method without Pivot Limit

is attained 95% of the time. Graphs summarizing the results are shown in Appendix D.

## B. PIVOTS REQUIRED

The number of pivots required by the spherical triangle method is shown in Figure 17. The mean number of pivots required is 1.73 and more than 2 pivots are rarely required. Since the spherical triangle method requires three stars before a pivot can occur, the average number of stars required by this method is 4.73. Since only a small number of attitudes require more than 4 pivots, the time efficiency of the method might be improved by limiting the number of pivots required to 3. The downside to this is that some of the attitudes requiring a great number of pivots are successfully identified, and as a result, the overall success of them for this method may drop slightly.

## C. CPU TIME REQUIRED

The CPU time required for the spherical triangle method is shown in Figure 18. It should be noted that solutions that take 20 seconds or more are grouped together into the 20 second slot. Some of the attitudes take as long a 400 seconds, resulting when more than 20 stars are within the FOV. Under these conditions, a thousand or more spherical triangles exist in the FOV and have to be sorted for pivoting. The average time required is 10.43 seconds. It is interesting to note that the median is 1.97 seconds and can be seen as the peak in the chart. For half of the attitudes tested, the result (correct, inconclusive, or otherwise) is given in 1.97 seconds or less, however, the other half took substantially longer, moving the average significantly to the right of the median. A surprising result is that a large percentage of attitudes that took 20 seconds or longer still resulted in a correct result; abandoning attitudes that are “taking too long” reduces the overall rate of success and would not be a good method to improve the CPU rate.

An alternative, suggested in the previous section, that limits the number of pivots to 3 may improve the time results. This has been tested, but the resulting graphs look very much like the results without pivot limits and are not included here. Graphs summarizing the results are shown in Appendix E. The overall success rate remains 92%. The average time drops significantly to 1.65 seconds, an 84% improvement. The median moves only slightly to 1.33 seconds. Since the number of pivots is limited, the average number of pivots drops to 1.29 pivots, meaning only an average of 4.29 stars are required.

## D. FALSE STAR INCLUSION

If a false star is added to the FOV, the spherical triangle method, like the angle method, has a much more difficult time reaching a solution, as shown in Figure 19. The overall success rate drops to 52% and 10%

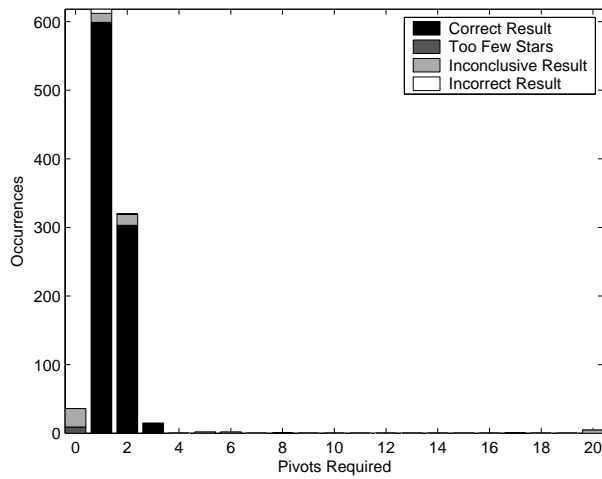


Figure 17. Pivots Required for Spherical Triangle Method without Pivot Limit

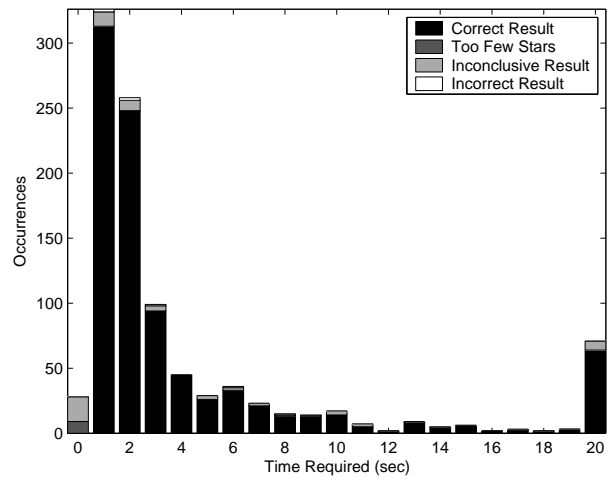


Figure 18. CPU Time Required for Spherical Triangle Method without Pivot Limit

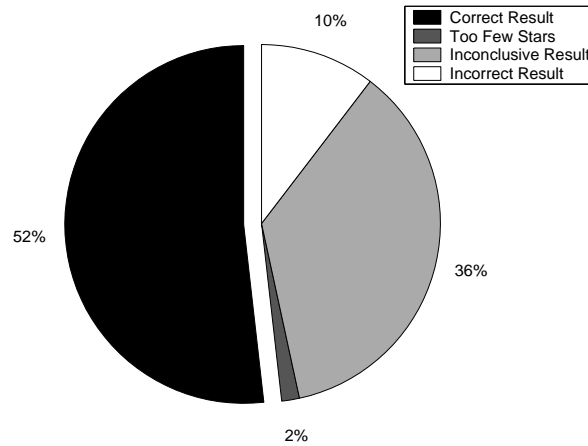


Figure 19. Spherical Triangle Method Results With a False Star in the FOV

of the results are incorrect. Like the angle method, if the pivot order happens to include the false star, the spherical triangle method cannot reach the correct result and will either approach the wrong solution or no solution at all. Graphs summarizing the results are shown in Appendix F.

## VIII. SUMMARY OF RESULTS

A summary of the results between the angle method and spherical triangle method is shown in Table 2. The angle method is limited to 9 pivots and the spherical triangle method is limited to 3 pivots. Being able to match the stars in the celestial sphere to those seen the star tracker's FOV using more than one property can result in a very fast recognition algorithm with a high rate of success. For a star tracker with an 8 deg FOV, sensitive to magnitude 6.0 stars, the spherical triangle method is almost twice as likely to be successful in identifying stars than the angle method. With appropriate pivot limits placed on both methods to minimize the response times without significantly sacrificing the rate of successful results, the spherical triangle method achieves a solution 4 times faster than the angle method. Just as important, the spherical triangle method achieves greater success using fewer stars than the angle method. The spherical triangle method, on average, examines only 4.29 stars versus the angle method's 6.86, which is a 37% improvement. It should be noted, however, that while the spherical triangle method is far more successful than the angle

**Table 2. Angle Method Vs. Spherical Triangle Method**

Item	Angle	Sph. Tri.
Minimum Stars Required	2	3
Min. Stars Req'd for Success	3	4
Overall Success Rate	55%	92%
Inconclusive Result	45%	6%
Incorrect Result	< 1%	< 1%
Average No. Pivots Required	4.86	1.29
Average No. Stars Required	6.86	4.29
Average CPU Time Required	6.89 sec	1.65 sec
False Star Correct Result	25%	52%
False Star Inconclusive Result	59%	36%
False Star Incorrect Result	17%	10%

method at identifying stars, it will only work when there are more than three stars in the FOV. The angle method only requires 3 stars before it starts to work, but even then, the angle method can only identify stars a small percentage of the time. For a star tracker sensitive to magnitude 6.0 stars and using an 8 degree FOV, attitudes with less than four stars in the FOV rarely happen, so this is not a significant issue.

Both methods have similar amounts of incorrect results when a false star is added to the star tracker's FOV, due to the  $3\sigma$  bound on the angle and spherical triangle searches. With such bounds, it is expected that 0.3% of the stars will be determined incorrectly, since, in those situations the correct solution lies outside the bounds of the search. If a false star is added to the star tracker's FOV, success rates from both methods suffer, but the spherical triangle method suffers less. It is able to correctly determine the stars in the FOV twice as often as the angle method and incorrectly identifies the stars in the FOV 60% as often. This is due to the fact the fewer stars are required to determine the stars in the FOV and so the spherical triangle method is less likely to start with or pivot to the false star. It is interesting to note that the spherical triangle method has almost the same overall success with a false star in the FOV as the angle method does without it.

The spherical triangle method is computationally intensive, but can find a result with only a few pivots a very large percentage of the time. Determining the order for pivoting requires a large portion of the CPU time, particularly for the spherical triangle method because combinations of three stars have to be examined as opposed to combinations of two stars required by the angle method. Since the number of pivots for the spherical triangle method can be limited to three without significantly affecting the results, the average CPU time required dramatically drops. The angle method can only be limited to 9 pivots before impacting the results and so cannot benefit as much. The price for speed is certainly storage. Requiring 167 MB, the spherical triangle catalog, including the  $k$ -vector array, is more than ten times larger than that required for the angle method. Methods for data storage aboard spacecraft are constantly improving and perhaps in the not-too-distant future (if not already), this size database will not be a significant issue.

## IX. CONCLUSIONS

A new approach for star pattern recognition has been developed using spherical triangles that incorporates area and polar moments to effectively identify stars. The approach presented here tackles the worst-case scenario for a star tracker: no a priori attitude information and no other sensor information to assist the identification process. Simulation results indicated that the spherical triangle method is almost twice as likely to be successful in identifying stars and achieves greater success using fewer stars than the angle method. Furthermore, the spherical triangle method is less sensitive to false star problems than the angle method.

## Appendix A Angle Method Without Pivot Limits

Figure 20 shows the results of the angle method without a pivot limit.

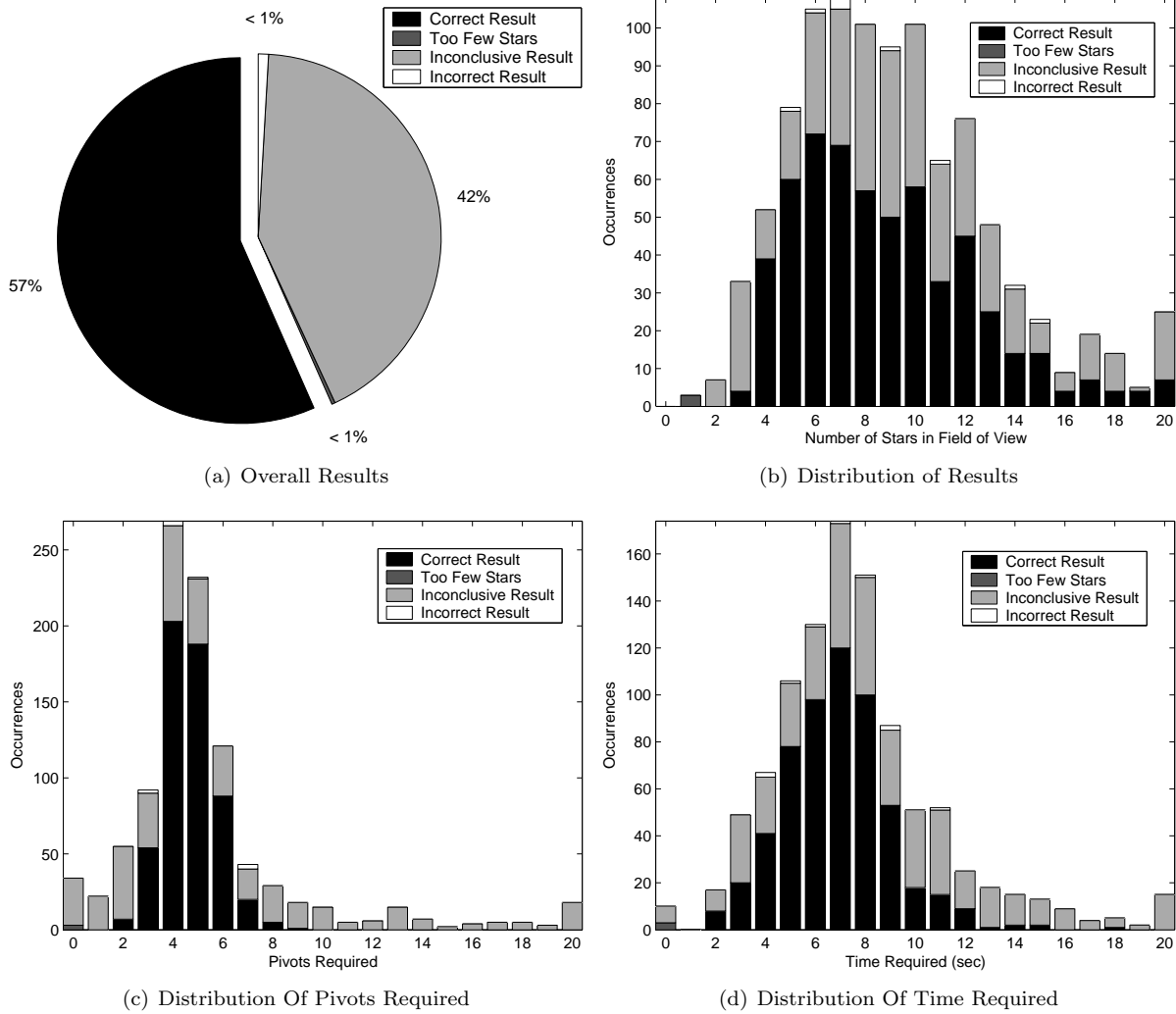


**Figure 20. Results of Angle Method Without Pivot Limit**

## Appendix B Angle Method With 9-Pivot Limits

Figure 21 shows the results of the angle method with a 9-pivot limit.

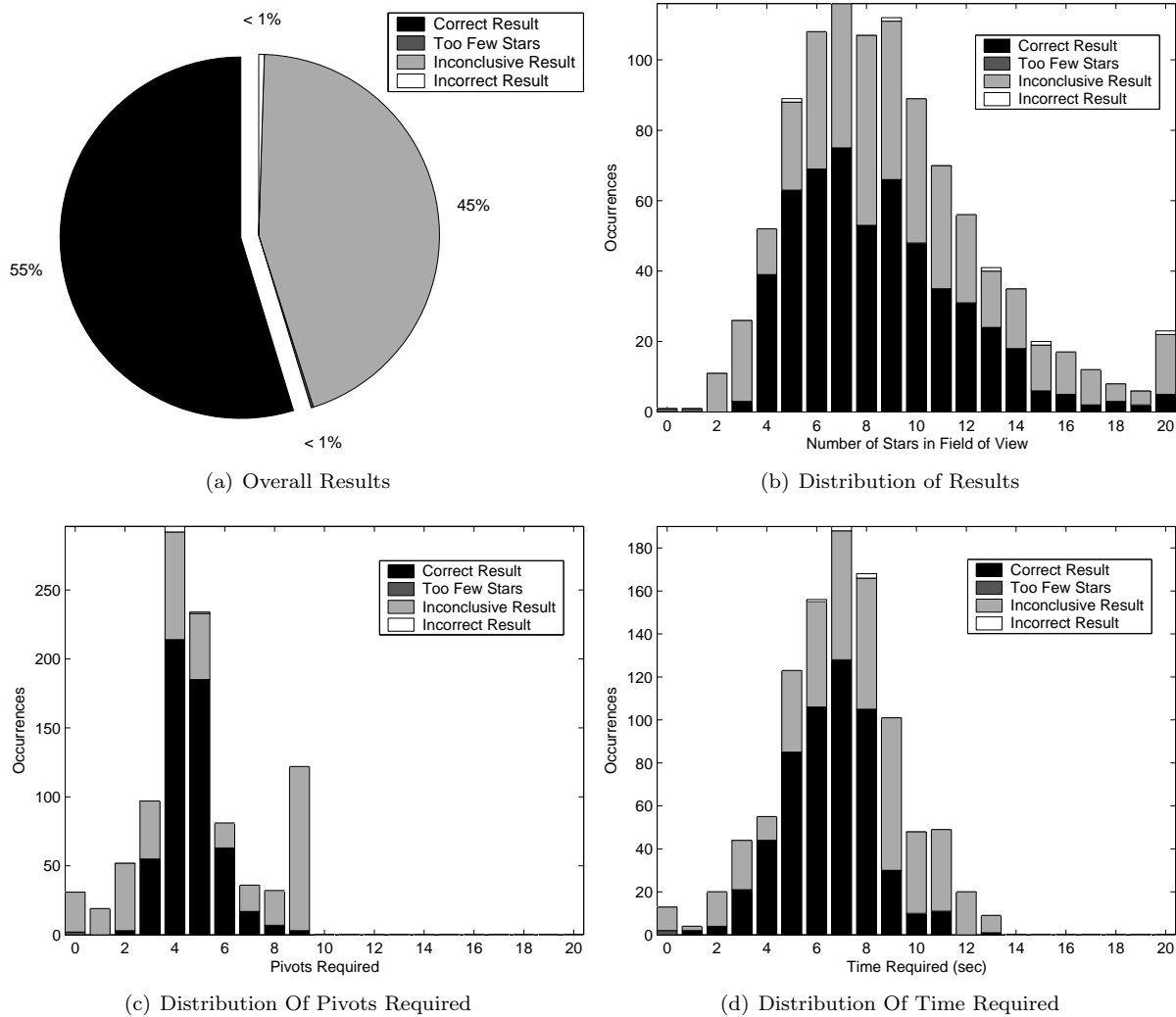
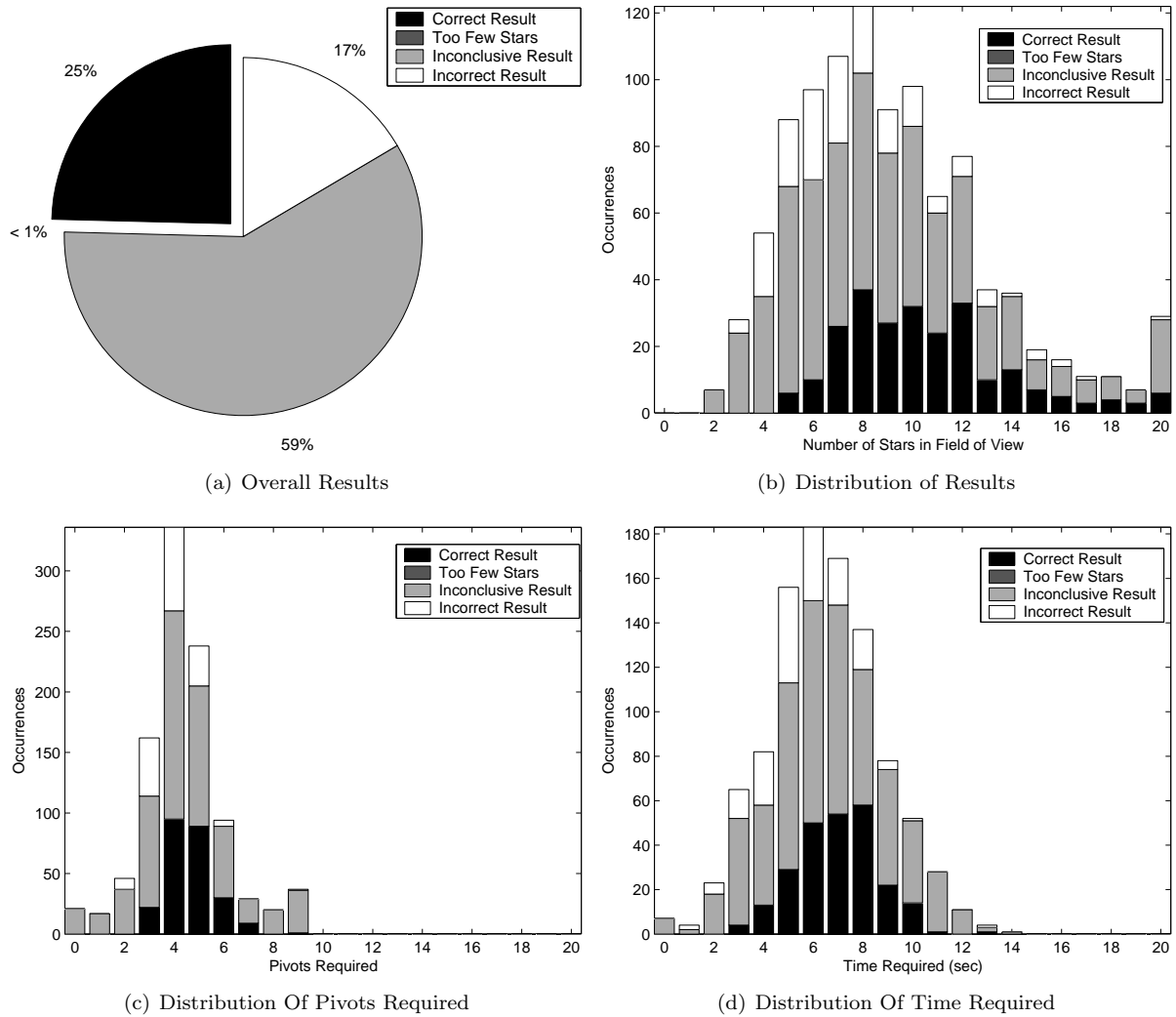


Figure 21. Results of Angle Method With a 9-Pivot Limit

## Appendix C

### Angle Method Including A False Star

Figure 22 shows the results of the angle method (9-pivot limit) with a false star added to the FOV. Note that the number of stars indicated in the FOV includes the false star.



**Figure 22. Results of Angle Method (9-pivot limit) Including a False Star**

## Appendix D Spherical Triangle Method Without Pivot Limits

Figure 23 shows the results of the spherical triangle method without a pivot limit.

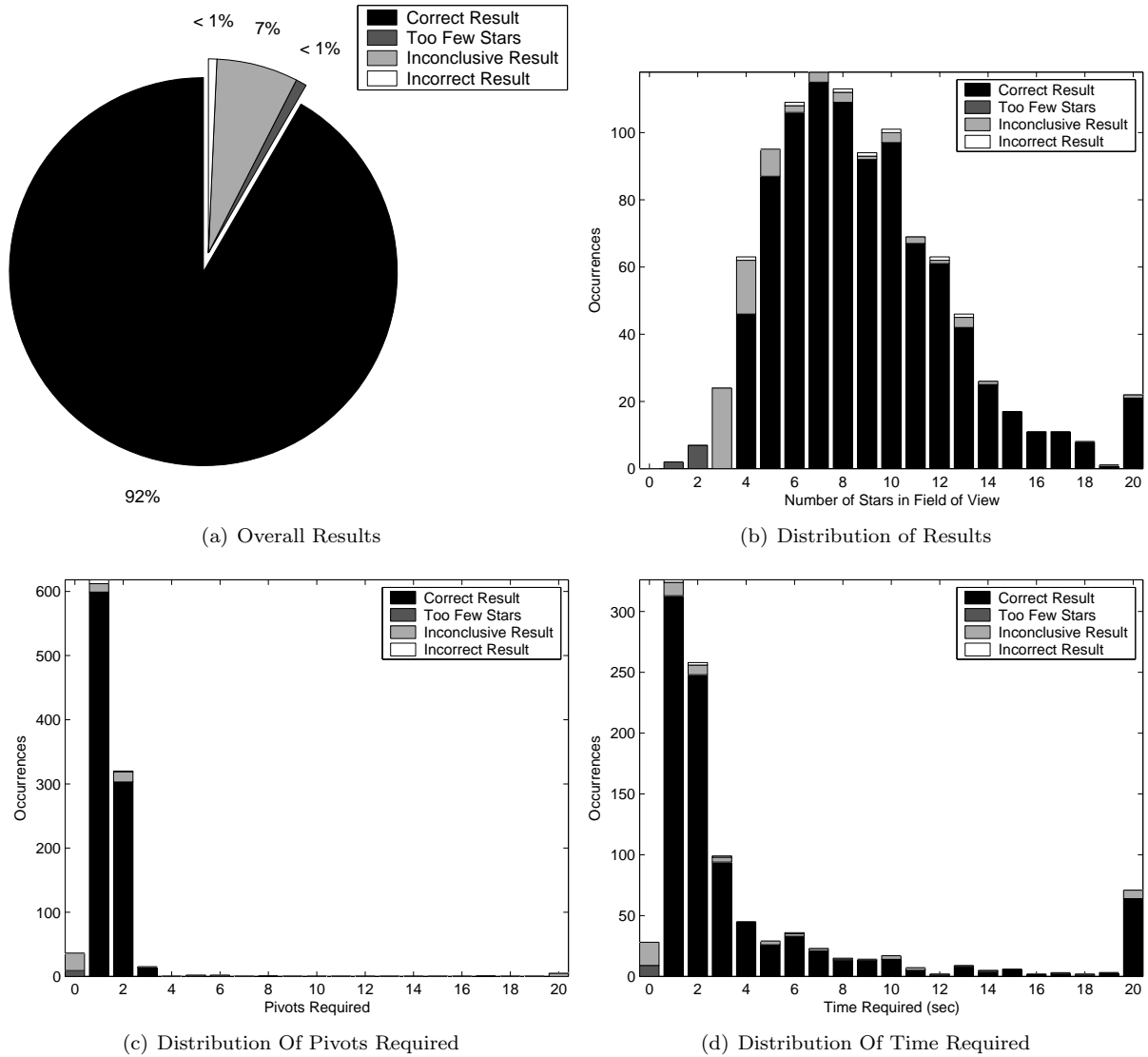


**Figure 23. Results of Spherical Triangle Method Without Pivot Limits**

## Appendix E

### Spherical Triangle Method With 3-Pivot Limit

Figure 24 shows the results of the spherical triangle with a 3-pivot limit.

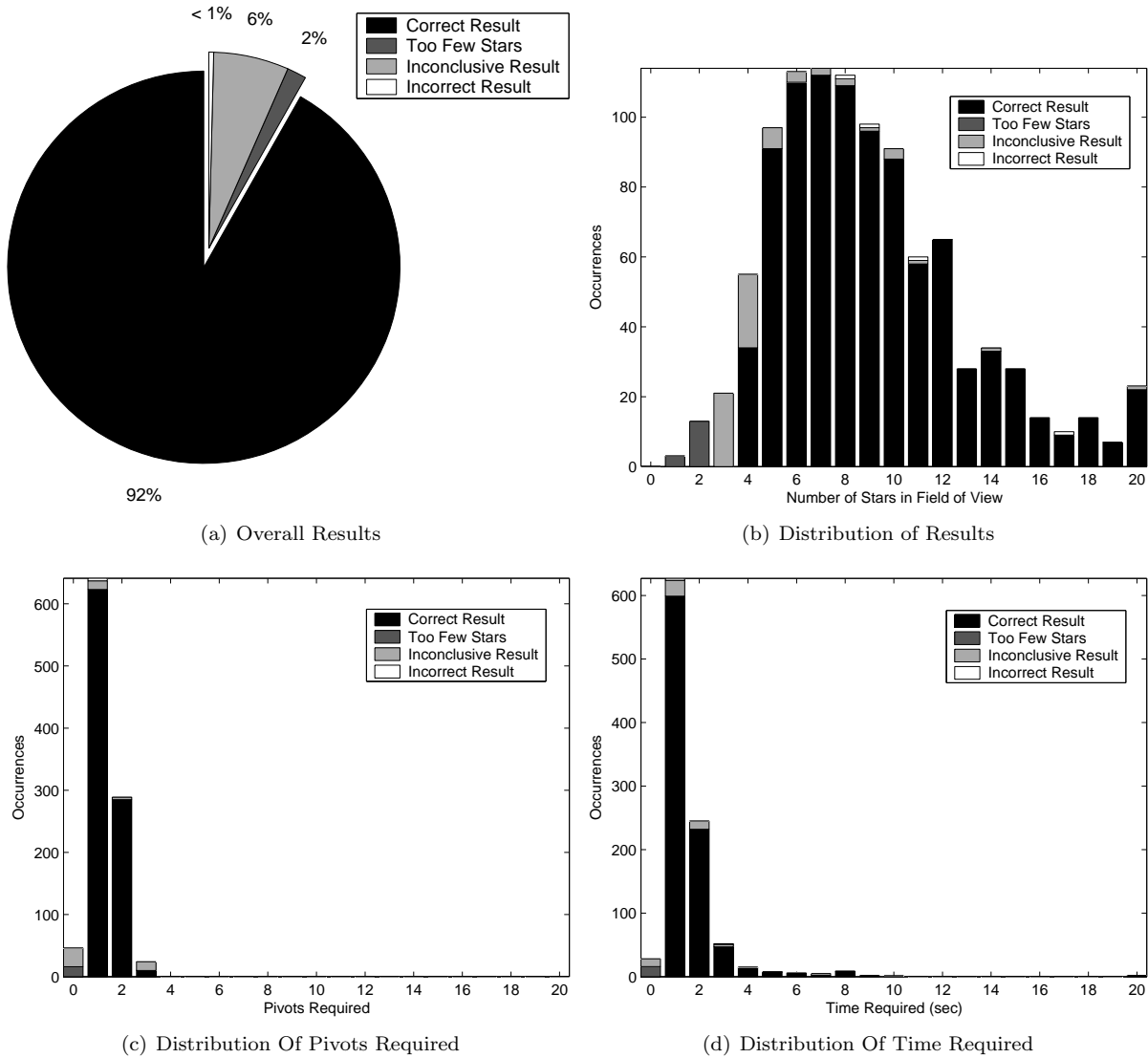


**Figure 24. Results of Spherical Triangle Method With 3-Pivot Limit**

## Appendix F

### Spherical Triangle Method Including A False Star

Figure 25 shows the results of the spherical triangle method (3-pivot limit) with a false star added to the FOV. Note that the number of stars indicated in the FOV includes the false star.

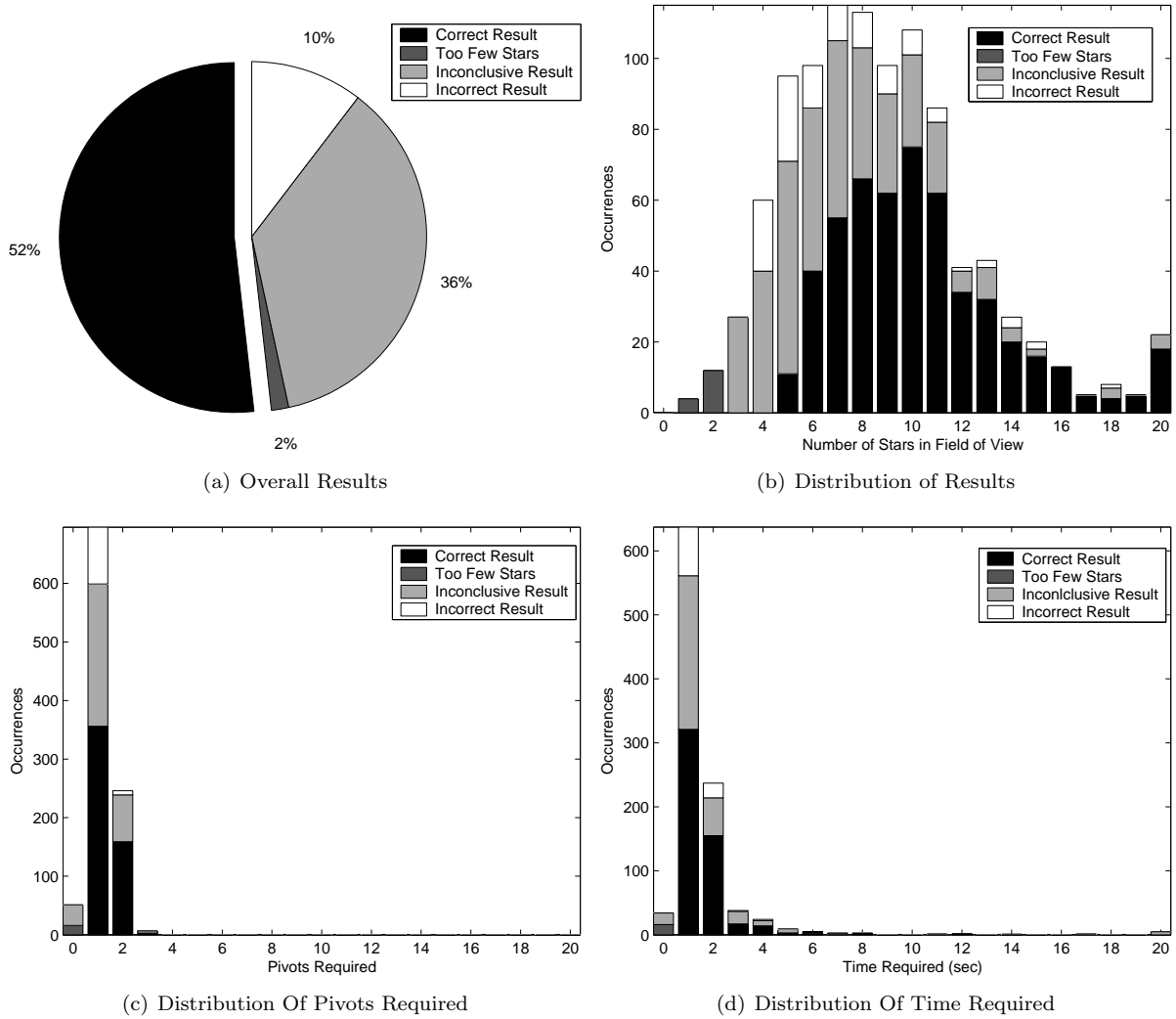


**Figure 25. Results of Spherical Triangle Method (3-pivot limit) Including a False Star**

## References

- <sup>1</sup>Ju, G. and Junkins, J. L., "Overview of Star Tracker Technology and its Trends in Research and Development," *Advances in the Astronautical Sciences, The John L. Junkins Astrodynamics Symposium*, Vol. 115, 2003, pp. 461–478, AAS 03-285.
- <sup>2</sup>Gottlieb, D. M., "Star Identification Techniques," *Spacecraft Attitude Determination and Control*, 1978, pp. 259–266.
- <sup>3</sup>Ketchum, E. A. and Tolson, R. H., "Onboard Star Identification Without A Priori Attitude Information," *Journal of Guidance, Control and Dynamics*, Vol. 18, No. 2, March-April 1995, pp. 242–246.
- <sup>4</sup>Kosik, J. C., "Star Pattern Identification Aboard an Inertially Stabilized Spacecraft," *Journal of Guidance, Control and Dynamics*, Vol. 14, No. 2, March-April 1991, pp. 230–235.
- <sup>5</sup>Gambardella, P., "Algorithms for Autonomous Star Identification," Tech. Rep. TM-84789, NASA, 1980.
- <sup>6</sup>Junkins, J. L., White, C. C., and Turner, J. D., "Star Pattern Recognition for Real Time Attitude Determination," *Journal of Astronautical Sciences*, Vol. 25, No. 3, Nov. 1977, pp. 251–270.
- <sup>7</sup>Junkins, J. L. and Strikwerda, T. E., "Autonomous Attitude Estimation via Star Sensing and Pattern Recognition," *Proceedings of the Flight Mechanics and Estimation Theory Symposium*, NASA-Goddard Space Flight Center, Greenbelt, MD, 1978, pp. 127–147.
- <sup>8</sup>Strikwerda, T. E., Junkins, J. L., and Turner, J. D., "Real-Time Spacecraft Attitude Determination by Star Pattern Recognition: Further Results," *AIAA Paper 79-0254*, January 1979.
- <sup>9</sup>Sheela, B. V., Shekhar, C., Padmanabhan, P., and Chandrasekhar, M. G., "New Star Identification Technique for Attitude Control," *Journal of Guidance, Control and Dynamics*, Vol. 14, No. 2, March-April 1991, pp. 477–480.
- <sup>10</sup>Williams, K. E., Strikwerda, T. E., Fisher, H. L., Strohhahn, K., and Edwards, T. G., "Design Study: Parallel Architectures for Autonomous Star Pattern Identification and Tracking," *AAS Paper 93-102*, Feb. 1993.
- <sup>11</sup>Ball Aerospace Systems Group, Electro-Optics Cryogenics Division, Boulder, CO, *Specification Sheet for Ball Aerospace CT-601 Star Tracker*.
- <sup>12</sup>Cole, C. L., *Fast Star Pattern Recognition Using Spherical Triangles*, Master's thesis, State University of New York at Buffalo, Buffalo, NY, Jan. 2004.
- <sup>13</sup>Mortari, D., "A Fast On-Board Autonomous Attitude Determination System Based on a New Star-ID Technique for a Wide FOV Star Tracker," *Advances in the Astronautical Sciences, Sixth Annual AIAA/AAS Space Flight Mechanics Meeting*, Vol. 93, Pt. 2, 1996, pp. 893–903, AAS 96-158.
- <sup>14</sup>Crassidis, J. L., Markley, F., Kyle, A., and Kull, K., "Attitude Determination Improvements for GOES," *Proceedings of the Flight Mechanics/Estimation Theory Symposium*, NASA-Goddard Space Flight Center, Greenbelt, MD, May 1996, pp. 151–165.
- <sup>15</sup>Shuster, M. D., "Maximum Likelihood Estimation of Spacecraft Attitude," *The Journal of the Astronautical Sciences*, Vol. 37, No. 1, Jan.–March 1989, pp. 79–88.
- <sup>16</sup>Jansen, J. D., "Use of Spherical Trigonometry to Compute Near-Well Flow Through Irregular Grid Block Boundaries," *Computational Geosciences*, Vol. 6, 2002, pp. 195–206.
- <sup>17</sup>Crassidis, J. L. and Junkins, J. L., *Optimal Estimation of Dynamic Systems*, Chapman & Hall/CRC, Boca Raton, FL, 2004, pp. 285–289.
- <sup>18</sup>Shuster, M. D., "Uniform Attitude Probability Distributions," *to appear in Journal of the Astronautical Sciences*, Vol. 51, No. 4, 2003.